



ELSEVIER

Available online at [www.sciencedirect.com](http://www.sciencedirect.com)**ScienceDirect**journal homepage: [www.elsevier.com/locate/he](http://www.elsevier.com/locate/he)

# Numerical simulation and consequence analysis of accidental hydrogen fires in a conceptual offshore hydrogen production platform

Hong Lin <sup>a,b,\*</sup>, Haochen Luan <sup>a</sup>, Lei Yang <sup>c</sup>, Chang Han <sup>a</sup>, Shuo Zhang <sup>a</sup>,  
Hongwei Zhu <sup>b</sup>, Guoming Chen <sup>b</sup>

<sup>a</sup> College of Pipeline and Civil Engineering, China University of Petroleum (East China), Qingdao, China

<sup>b</sup> Center for Offshore Engineering and Safety Technology (COEST), China University of Petroleum (East China),  
Qingdao, China

<sup>c</sup> College of Science, China University of Petroleum (East China), Qingdao, China

## HIGHLIGHTS

- Simulation of hydrogen fire for a conceptual offshore hydrogen production platform.
- Effect of facilities layout, leakage velocity and direction on fire consequences.
- Suppression effects of firewall with different height on hydrogen fires.

## ARTICLE INFO

### Article history:

Received 5 August 2022

Received in revised form

6 November 2022

Accepted 30 November 2022

Available online 28 December 2022

### Keywords:

Offshore hydrogen production  
platform

Hydrogen fire

Non-premixed combustion

CFD model

Numerical simulation

## ABSTRACT

At present there exist many abandoned offshore platforms which could be transformed into hydrogen production platforms helping to reduce the cost of hydrogen production. In this study, the potential fire caused by hydrogen leakage in a large-scale hydrogen production platform was simulated and the consequence was analyzed by Computational Fluid Dynamics (CFD) numerical simulation. The uniqueness of this research lies in establishing an overall platform model and considering the influences of facility layout, leakage location, and leakage velocity on the combustion process of hydrogen fire. Moreover, the suppression effects of a firewall with different height on hydrogen fires were compared. The results show that the layout of facilities will affect the temperature distribution. Due to poor ventilation, high temperature appears in congested areas with facilities. The increase of leakage velocity leads to the expansion of high temperature area, also, firewall could protect key facility from high temperature effectively.

© 2022 Hydrogen Energy Publications LLC. Published by Elsevier Ltd. All rights reserved.

## Introduction

As a kind of clean and renewable energy, hydrogen is being further developed and utilized in recent years [1,2]. Green

hydrogen, which was produced by water electrolysis technology, has more promising prospects in utilization due to its advantage of friendly environmental and this leads to the requirement to develop the more efficient facilities for green hydrogen production and storage [3,4]. The viability of

\* Corresponding author.

E-mail address: [linhong@upc.edu.cn](mailto:linhong@upc.edu.cn) (H. Lin).

<https://doi.org/10.1016/j.ijhydene.2022.11.349>

0360-3199/© 2022 Hydrogen Energy Publications LLC. Published by Elsevier Ltd. All rights reserved.

**Nomenclature**

$c$	specific heat , J/kg·K
$D$	molecular diffusivity , m <sup>2</sup> /s
$E$	total energy, J/kg
$G_b$	generation of kinetic energy due to buoyancy , kg/ms <sup>-3</sup>
$G_k$	generation of kinetic energy due to mean velocity Gradients , kg/ms <sup>-3</sup>
$\delta_{ij}$	Kronecker symbol
$\varepsilon$	energy dissipation rate , m <sup>2</sup> /s <sup>3</sup>
$\mu$	dynamic viscosity , Pa·s
$\bar{\rho}$	average density of gas components , kg/m <sup>3</sup>
<i>Subscripts</i>	
$g$	gravity acceleration , m/s <sup>2</sup>
$h$	Enthalpy , J/kg
$k$	turbulent kinetic energy , m <sup>2</sup> /s <sup>2</sup>
$M$	Mach number , -
$Pr$	Prandtl number , -
$p$	pressure , Pa
$R_m$	source term , kg/m <sup>3</sup> /s
$S$	source term , -
$Sc$	Schmidt number , -

$E$	energy
$eff$	effective
$i,j,k$	spatial coordinate indexes
$m$	index of chemical species
$p$	pressure
$t$	turbulent
<i>Constants and model parameters</i>	
$S_k$	source term , -
$T$	temperature , K
$t$	time , s
$\tilde{u}_{i,j,k}$	velocity components , m/s
$x_{i,j,k}$	spatial coordinates , m
$C_{1e}$	1.42
$C_{2e}$	1.68
$C_{3e}$	tanh  $\omega/u $
<i>Bars</i>	
$Y$	mass fraction ,
-	Reynolds averaged parameters
$\sim$	Favre averaged parameters
<i>Greek</i>	
$\alpha$	inverse effective Prandtl number

offshore wind to provide green hydrogen is a hot topic in recent years, and there has been increasing interest in coupling offshore wind with hydrogen production [4]. At present, one of the feasible schemes for hydrogen production is to use semi-submersible floating offshore wind (FOW) platform to produce hydrogen. This scheme is adopted in the Dolphin (Deepwater Offshore Local Production of HYdrogeN) project promoted by ERM, a company in Aberdeen, UK, and expected to be accomplished at Mid 2030s [5]. Meanwhile, using the existing aged oil and gas production platform to produce hydrogen is another more feasible scheme [6,7]. In early July 2019, the Q13 a - A offshore platform of Neptune Energy of the Netherlands was selected to carry out the world's first offshore hydrogen production project named PosHYdon [7].

As known, there are some important facilities for green hydrogen production and storage in an offshore hydrogen production system. Here, a conceptual offshore hydrogen production platform transformed from a jacket platform is illustrated in Fig. 1, with important facilities including electrolyser, water purification system, hydrogen storage tank, hydrogen supply pipes, and so on. Nevertheless, the above research is presently under way, lots of foundation knowledge about the offshore hydrogen production platform need to be studied.

During the long-term operation of the offshore platform in harsh conditions at ocean, there is a great potential risk of leakage of hydrogen caused by sudden crack or fracture to hydrogen supply pipes or hydrogen storage tanks, due to corrosion, vibration, collision and even human factors. Moreover, as one kind of flammable and explosive gas, hydrogen is easy to cause fire accidents if it leaks from supply pipes or storage tanks [8]. Once the hydrogen fire occurs, the heat radiation will both be the direct reason for fatalities and

personnel injuries. At the same time, the leaked hydrogen gas mix with air to form a large-scale combustible cloud with further risk of explosion or detonation [9,10]. As the most destructive accident scenarios, hydrogen explosion will cause devastating damage to the platform structure due to the high temperature and overpressure, which will further aggravate the spread of hydrogen fire. Therefore, considering the hydrogen fire posing a great threat to both asset integrity and human life, the improved knowledge of dispersion and combustion of hydrogen fire is of great importance for safety design, risk mitigation and prevention of the platform before it could be transformed for hydrogen production.

Up to now, a lot of progress have been achieved about the fire caused by combustion fuels, such as natural gas, especially methane, which focused on the behavior of gas diffusion and fire development [11–13]. However, compared with methane, hydrogen has higher calorific value and lower density, which leads to faster diffusion and more heat release of hydrogen in open environment. Moreover, due to its chemical

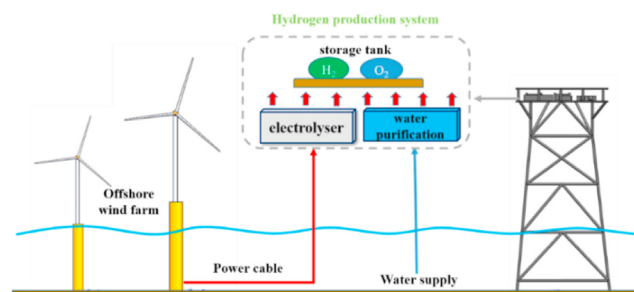


**Fig. 1 – A conceptual offshore hydrogen production platform in the ocean.**

characteristics, hydrogen is prone to blast in fire once the explosion limit conditions are reached, which makes the hydrogen fire more dangerous than methane fire [14].

In the past years, a number of experimental studies on hydrogen leakage and hydrogen fire have been done [15–18]. Most of tests on hydrogen fire behavior are mainly focus on the ignition test and model validation on simple geometries. In the previous studies (Schefer et al., 2006 [15]), measurements were performed in large-scale, vertical flames to characterize the dimensional, thermal, and radiative properties of ignited hydrogen jets. Giannissi et al. [19] experimentally examined hydrogen's leakage and diffusion behaviors under natural ventilation conditions.

In recent years, numerical simulation has become a powerful tool to investigate the leakage and combustion of hydrogen in actual hydrogen fire scenarios, due to its advantages of low risk, low cost, and high computational efficiency. With the help of CFD (Computational Fluid Dynamics) based model, there are lots of numerical studies on prediction of the hydrogen fire action. Molkov et al. [20,21] have conducted a lot of researches related to hydrogen jet fires in passively ventilated enclosure. Numerical experiments are performed to understand different regimes of hydrogen non-premixed combustion in an enclosure with passive ventilation through one horizontal or vertical vent located at the top of a wall. Considering hydrogen being transported by a truck, Gu et al. [22] investigated the temperature distribution and hydrogen concentration at different stages of a hydrogen jet fire. Takeno et al. [23] performed tests and conducted numerical simulations in a 40-MPa hydrogen cylinder for examining the induced leakage, diffusion and explosion. At present, different CFD codes, e.g. ANSYS/FLUENT (Molkou and Shentsov, 2014 [20]), FDS (Yuan et al., 2021 [24]), FLACS (Kim et al., 2013 [25]), ANSYS/CFX (Schmidt et al., 1999 [26]), fireFoam (Bauwens & Dorofeev, 2014 [27]; Ouyang et al., 2020 [28]) have been developed for simulation of hydrogen diffusion, fire or explosion. Except for the software mentioned above, a Sandia FUEGO code [29] was developed at Sandia National Laboratories to characterize and predict the behavior of unintended hydrogen releases. The above research shows that, it is reliable and meaningful to use CFD software to investigate the leakage and combustion of hydrogen in actual hydrogen fire scenarios.

Moreover, the protection of structures and facilities in fire is also one of the focuses of hydrogen fire researches (Kuroki et al. [30], Yuan [24]). In 2011, Willoughby and Royle [31] studied the influence of wall barriers on separation distance from hydrogen high pressure horizontal jet fires. Kuroki et al. [23] focused on two types of hydrogen-gasoline hybrid refueling stations, and a risk assessment study on thermal radiation is carried out with a fire at each hybrid station. Based on analysis, it had been found that the container walls can greatly insulate the radiative flux. Yuan [24] evaluated the reliability of a fine water mist for the suppression of fires on hydrogen fuel cell ships by using FDS software.

As described above, scholars have made a lot of meaningful explorations regarding the leakage and combustion of hydrogen for some actual engineering, such as buildings, hydrogen fueling station, hydrogen fuel cell ships and hydrogen storage tanks. However, to the best authors'

knowledge, there is few researches on the offshore platform hydrogen fire with the feature of occurring in large-scale open ambient air. Moreover, a conceptual offshore hydrogen production platform significantly differs from the previous objects in the spatial size, layout, environmental condition and ventilation condition. Thus, the knowledges and results from previous studies cannot provide direct and sufficient guidance to the hydrogen's diffusion and combustion behaviors on an offshore hydrogen production platform.

Thus, considering offshore hydrogen production platforms will serve as an important and expected hydrogen production and storage infrastructure, simulation of various potential fire scenarios will be required to be carried out and analyzed, so as to provide guidance for safety design and ensure the safety of facilities and personnel on platform. This paper aims at understanding of hydrogen fires on a large-scale offshore hydrogen production platform, in which the hydrogen combustion behaviors and fire development characteristics in actual scenarios are addressed by using ANSYS Fluent software. The uniqueness of this research lies in establishing a numerical model of the overall platform and considering the influences of facility layout, leakage location, and leakage velocity on the combustion process of hydrogen fire. Moreover, the suppression effects of a firewall with different height on hydrogen fires were compared and analyzed. The study will contribute to the safety design of offshore hydrogen production offshore platforms, and promote the functional transformation of abandoned offshore platforms.

## Methodology and validation

### CFD methodology

#### Governing equations of fluid dynamics

The simulation of fire combustion is calculated based on the governing equations, including conservation of mass, momentum, energy and species, as follows [20].

$$\frac{\partial \bar{\rho}}{\partial t} + \frac{\partial}{\partial x_j} (\bar{\rho} \tilde{u}_j) = 0 \quad (1)$$

$$\frac{\partial \bar{\rho} \tilde{u}_i}{\partial t} + \frac{\partial}{\partial x_j} (\bar{\rho} \tilde{u}_j \tilde{u}_i) = - \frac{\partial \bar{p}}{\partial x_i} + \frac{\partial}{\partial x_j} (\mu + \mu_t) \left( \frac{\partial \tilde{u}_i}{\partial x_j} + \frac{\partial \tilde{u}_j}{\partial x_i} - \frac{2}{3} \frac{\partial \tilde{u}_k}{\partial x_k} \delta_{ij} \right) + \bar{\rho} g_i \quad (2)$$

$$\begin{aligned} \frac{\partial}{\partial t} (\bar{\rho} \tilde{E}) + \frac{\partial}{\partial x_j} (\tilde{u}_j (\bar{\rho} \tilde{E} + \bar{p})) &= \frac{\partial}{\partial x_j} \left( \left( k + \frac{\mu_t c_p}{Pr_t} \right) \frac{\partial \tilde{T}}{\partial x_j} \right. \\ &\quad \left. - \sum_m \tilde{h}_m \left( - \left( \rho D + \frac{\mu_t}{Sc_t} \right) \frac{\partial \tilde{Y}_m}{\partial x_j} \right) \right. \\ &\quad \left. + \tilde{u}_i (\mu + \mu_t) \left( \frac{\partial \tilde{u}_i}{\partial x_j} + \frac{\partial \tilde{u}_j}{\partial x_i} - \frac{2}{3} \frac{\partial \tilde{u}_k}{\partial x_k} \delta_{ij} \right) \right) + S_E \end{aligned} \quad (3)$$

$$\frac{\partial \bar{\rho} \tilde{Y}_m}{\partial t} + \frac{\partial}{\partial x_j} (\bar{\rho} \tilde{u}_j \tilde{Y}_m) = \frac{\partial}{\partial x_i} \left( \left( \rho D + \frac{\mu_t}{Sc_t} \right) \frac{\partial \tilde{Y}_m}{\partial x_i} \right) + R_m \quad (4)$$

where  $\bar{\rho}$  is the average density of gas components;  $t$  is time;  $x_{i,j,k}$  is the spatial coordinates;  $\tilde{u}_{i,j,k}$  is the velocity components;  $\mu$  is dynamic viscosity;  $g$  is gravity acceleration;  $E$  is energy;  $p$  is

pressure;  $k$  is turbulent kinetic energy;  $c$  is specific heat;  $\Pr$  is Prandtl number;  $T$  is temperature;  $h$  is enthalpy;  $D$  is molecular diffusivity;  $Sc$  is Schmidt number;  $Y$  is mass fraction;  $\delta_{ij}$  is Kronecker symbol;  $S$  is source term;  $R_m$  is the source term;  $i, j, k$  are spatial coordinate indexes;  $m$  is index of chemical species; Subscripts  $t$  is turbulent.

#### Turbulence model

In ANSYS Fluent, the transient pressure-based solver is used to simulate gas combustion in the gas domain. Compared with the steady-state solver, the transient solver estimated the behavior of the fire temperature over time more accurately. The renormalization group (RNG)  $k-\epsilon$  turbulence model is applied that was derived from the instantaneous Navier-Stokes equations. The analytical derivation resulted in a model with constants different from those in the standard  $k-\epsilon$  model, and additional terms and functions in the transport equations for  $k$  and  $\epsilon$ . Compared with the standard  $k-\epsilon$  model, RNG theory provides an analytical formula considering low Reynolds number flow viscosity, which has higher reliability and accuracy in a wider range of flows [32,33]. Transport equations for the turbulent kinetic energy,  $k$ , and the energy dissipation rate,  $\epsilon$ , in the RNG  $k-\epsilon$  turbulence model are [20]:

$$\frac{\partial}{\partial t}(\rho k) + \frac{\partial}{\partial x_i}(\rho k u_i) = \frac{\partial}{\partial x_j}\left(\alpha_k \mu_{eff} \frac{\partial k}{\partial x_j}\right) + G_k + G_b - \rho \epsilon - Y_M + S_k \quad (5)$$

$$\begin{aligned} \frac{\partial}{\partial t}(\rho \epsilon) + \frac{\partial}{\partial x_i}(\rho \epsilon u_i) &= \frac{\partial}{\partial x_j}\left(\alpha_\epsilon \mu_{eff} \frac{\partial \epsilon}{\partial x_j}\right) + C_{1\epsilon} \frac{\epsilon}{k} (G_k + G_{3\epsilon} G_b) - C_{2\epsilon} \rho \frac{\epsilon^2}{k} \\ &\quad - R_\epsilon + S_\epsilon \end{aligned} \quad (6)$$

where  $\alpha$  is inverse effective Prandtl number; eff is effective;  $G_k$  is generation of kinetic energy due to mean velocity Gradients;  $G_b$  is generation of kinetic energy due to buoyancy;  $\epsilon$  is energy dissipation rate;  $M$  is Mach number;  $S_k$  is source term;  $C_{1\epsilon}$  is constant 1.42;  $C_{2\epsilon}$  is constant 1.68;  $C_{3\epsilon}$  is constant  $\tanh|\omega|/u|$ .

#### Non-premixed combustion model

In previous studies, Eddy Dissipation Concept (EDC) model including chemical reaction mechanism in the species transport module was generally selected to simulate the combustion action. It assumes that combustion reactions occur in a small-scale turbulent structure. This model requires detailed setting of chemical reaction mechanism to ensure the accuracy of calculation results. Thus, it seems to be not suitable in practice especially for large models e.g. the offshore platform, since it takes a long calculating time and is difficult to be converged. Therefore, in this paper, the non-premixed combustion model is adopted to simulate the process of combustion. Reaction process is controlled by setting the mixture ratio of the combustion products. Chemical reaction mechanism is not considered in the combustion process. The state Relation is set as Chemical Equilibrium, and Energy Treatment is set as Non-Adiabatic. After determining the components of the leaked gas, the probability density function (PDF table) is generated. In the calculation process, some factors leading to energy loss such as heat radiation and heat flow at the air boundary are ignored. This causes the calculated temperature slightly higher than the real fire. But by this

way, a higher calculation efficiency can be achieved, which is more suitable for the combustion calculation for large-scale complex models of the offshore platform [34].

#### Validation study

In order to verify the correctness and accuracy of our proposed simulation methods of non-premixed combustion, the verification study of a jet fire caused by hydrogen release in a vented cube is carried out, which is consistent with the research made by Molkov et al. during 2014 [20]. Fig. 2 shows the numerical model established in this paper with the same size and conditions consistent with that of [20]. The calculation domain is divided into two parts including the solid domain of the box and the surrounding gas domain.

According to Ref. [20], case No.5 is selected to be verified. The vent is a vertical hole with the dimension of 30 cm × 3 cm. The  $H_2$  is leaked through a circular hole with the diameter of 5.08 mm and the release velocity of 60 m/s. Numerical calculations were performed using ANSYS Fluent, and the non-premixed combustion model is used to simulate the whole combustion behavior. The calculation process adopts pressure-based solver with SIMPLE pressure and velocity coupling algorithm and spatial discretization of the first order.

Fig. 2(b) and (c) shows the results of the verification simulation of our model and compares with the simulation of Molkov et al. [20]. It can be seen that the verified results are consistent with the results of Molkov et al. Comparing the shape of the flame, it could be found that the same pattern of the flame appears for both our simulation and the simulation of Molkov et al. during the development of hydrogen fire. Furthermore, comparison of the highest temperature between the results of our simulation and that of Molkov et al., shows that the maximum relative error is only 3.5%, which is acceptable due to the difference of grid division and calculation methods.

## Model establishment and fire scenarios setting

#### Description of the offshore hydrogen production platform

This study focused on a conceptual offshore hydrogen production platform which is transformed from a typical offshore oil and gas jacket platform. This is a four-legged jacket platform consisting of two-layer of deck. The diagram of the proposed offshore hydrogen production platform is shown in Fig. 3(a). The total height of the platform is 104 m, with the gap between two decks of 7 m. The two decks are designed with the same dimension, i.e. length is  $L = 50$  m, width is  $W = 50$  m, which was presented in Fig. 3(a).

The upper deck is designed for the rig, helicopter, the control compartment, etc., while the bottom deck was designed for hydrogen production system, composed of Hydrogen storage tank I, Hydrogen storage tank II, Compressor, High voltage transformer, Rectifier, and Seawater desalination system. The layout of facilities on the bottom deck on the offshore hydrogen production platform is illustrated in Fig. 3(b). Also, it was known that there exist some hydrogen supply pipelines in the hydrogen system, however they were not plotted in Fig. 3.

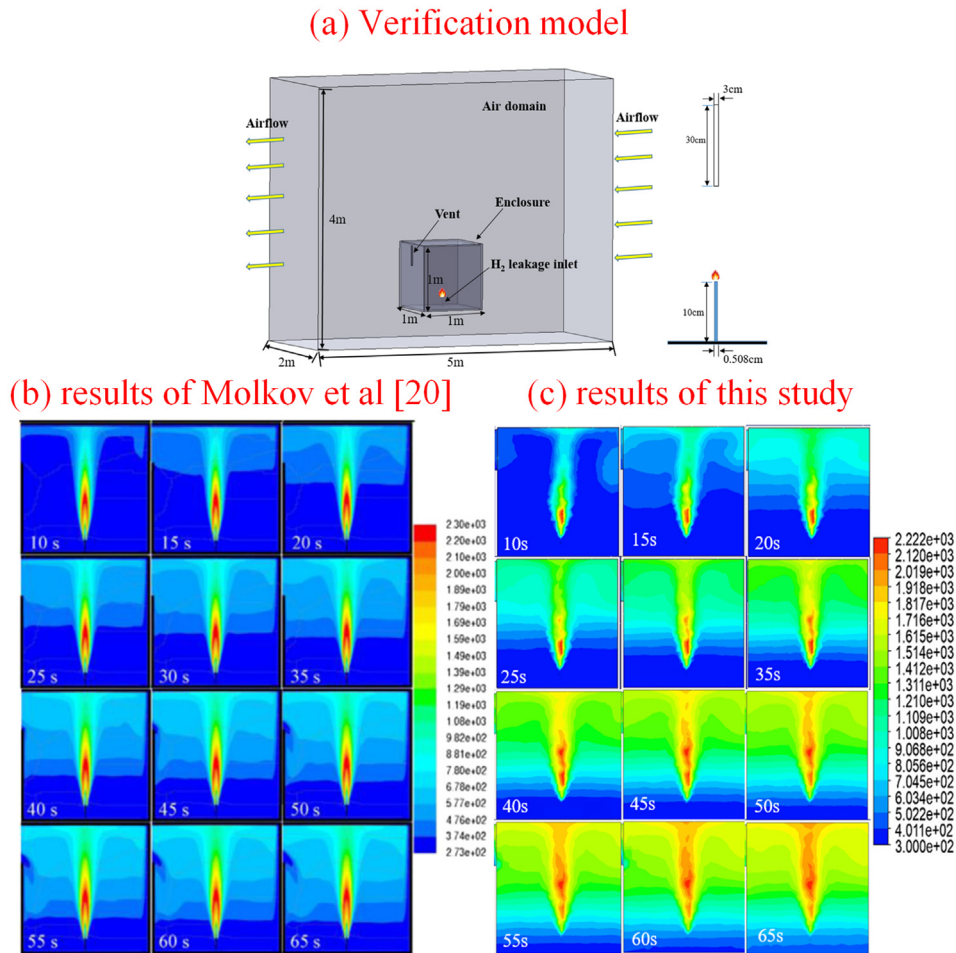


**Fig. 2 – Temperature slice along the enclosure centre-line in simulation (left: results of Molkov et al. [20]; right: results of this study).**

Here, it was assumed that hydrogen supply pipelines are distributed under Electrolytic bath and Seawater desalination system in Fig. 3, which could be regarded as posing great safety risks if hydrogen leakage occurred due to the sudden crack or fracture, or some human factors.

#### Calculation domain and boundary conditions

Considering the dimension of each deck is length of 50 m and width of 50 m, we choose the size of the entire calculation domain as  $L \times W \times H = 150 \text{ m} \times 150 \text{ m} \times 30 \text{ m}$ , which is 5 times the volume of the upper part of the jacket platform. Furthermore, to ensure the efficiency and the accuracy of the calculation, two different regions of the calculation domain is divided as shown in Fig. 4, in which the central region ( $L_1 \times W_1 \times H_1 = 75 \text{ m} \times 75 \text{ m} \times 25 \text{ m}$ ) is meshed using refined grids, while the outer domain is meshed using coarse grids.

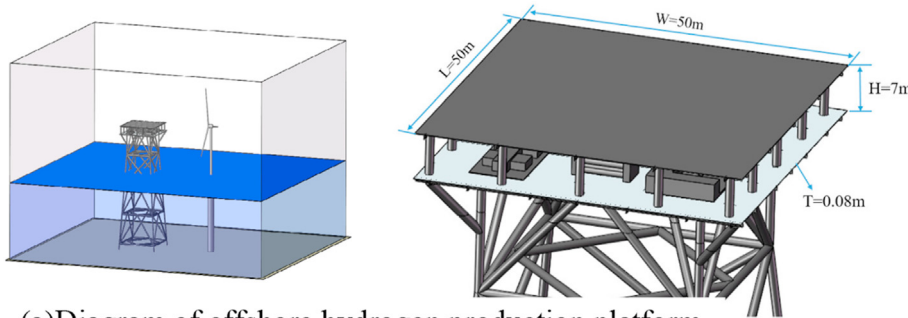
In the process of discretization, different sizes of grids are used to ensure the smooth convergence of the calculation process and to improve the accuracy of the results. Also, the computational efficiency was taken into account. Here, the grid cell size of the main body was set as 3 m, while the element size of the central encryption area of the platform was 0.45 m. In total, there are 2,190,985 nodes and 12,346,384

elements in the finite element model for subsequent simulation in this paper.

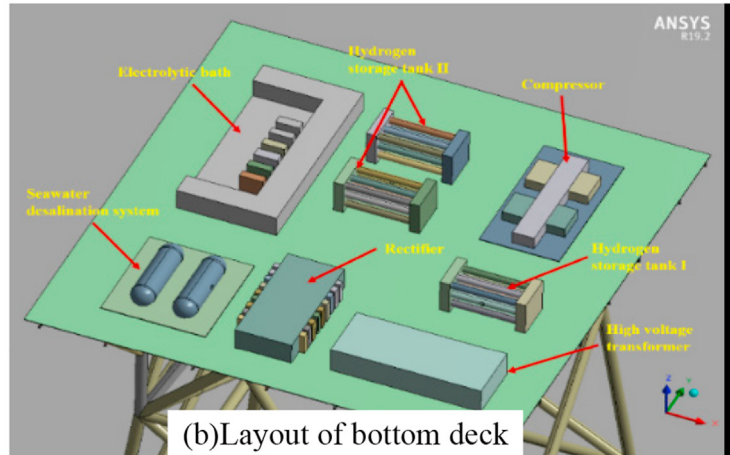
According to the previous description, the calculation domain in Fig. 4 is cut from the original calculation model. Therefore, all four surrounding boundaries including upper plane, bottom plane, two side planes are set as symmetric boundaries. The other two surfaces along to the X axis are provided with an air inlet and an air outlet, respectively (Fig. 4). The simulation was performed at an ambient temperature of 300 K, with a default ambient wind speed of 2 m/s at the air inlet, and a pressure-outlet at the air outlet. The illustration of the boundary conditions of the calculated domain are shown in Fig. 4. For all the fire scenarios to be simulated, it was assumed that the hydrogen storage tank or the pipeline on the bottom deck ruptured accidentally, and the hydrogen gas leaked was ignited instantly to form a jet fire. The simulating time for each scenario was set as 100s, and the temporal resolution of the numerical simulations were set as 0.1s for each time step.

#### Solution method in CFD

In Fluent, finite volume method is utilized to conduct a first order discrete of governing equations in Section CFD



(a)Diagram of offshore hydrogen production platform

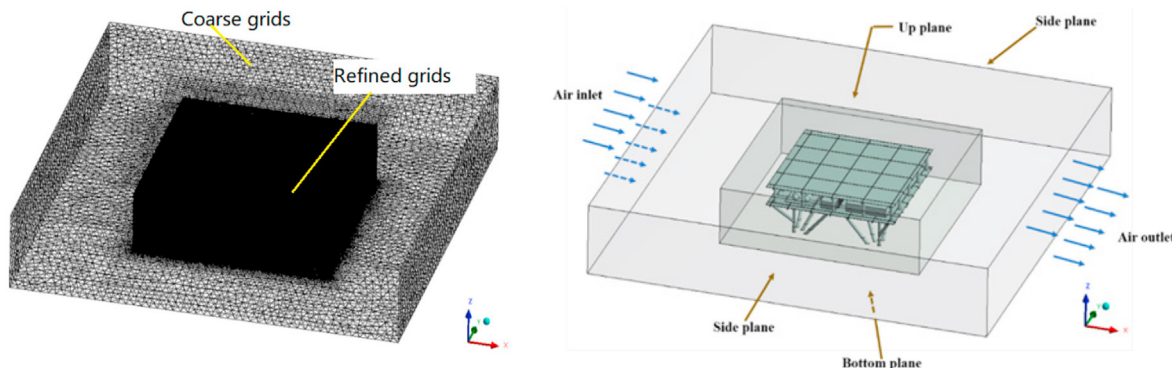
**Fig. 3 – Illustration of the proposed offshore hydrogen production platform.**

**methodology.** The transient pressure-based solver is used to simulate gas combustion in the gas domain. The SIMPLE algorithm is adopted for the pressure and velocity coupling schemes. The diffusion of leakage gas is an unsteady turbulence motion, therefore, the standard  $k-\epsilon$  model is chosen as the viscous model in the calculation process. The non-premixed combustion model is used to simulate the process of combustion.

#### Fire scenarios setting

As stated above in 3.1, both the fire scenarios caused by leakage from hydrogen storage tanks and hydrogen supply pipelines

are considered and investigated in this paper. As known, different leak locations and direction, diameters of leakage hole, flow rates, as well as equipment layout in fluid domain will have a great impact on the combustion consequences. Therefore, in this study, four leakage locations including Point A (leaked from pipeline at Electrolytic bath), Point B (leaked from pipeline at Seawater desalination system), Point C (leaked from Hydrogen storage tank I), and Point D (leaked from Hydrogen storage tank II), which were located at different positions are considered, as shown in Fig. 5(a). The leakage scenarios are listed in Table 1 as follows. The diameter of each leakage hole is 0.5 m. Three different flow rates of leakage are set including 10 m/s, 30 m/s, and 50 m/s, respectively.

**Fig. 4 – Grids (left) and boundaries (right) of the gas domain.**

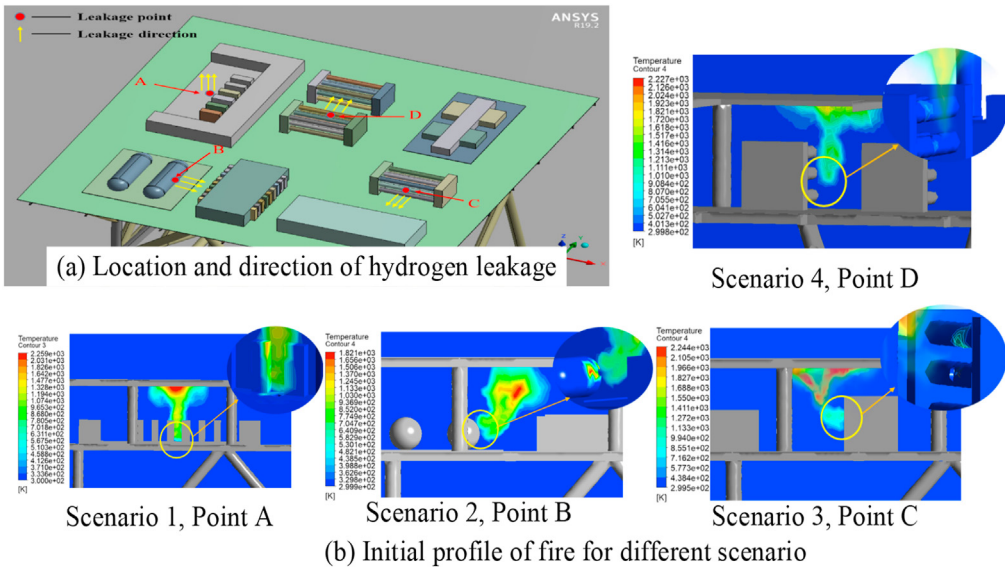


**Fig. 5 – (a) Location and direction of hydrogen and (b) Initial profile of fire for different scenario.**

## Results and discussion

### Fire development of different leakage scenarios

#### Initial fire profile of different leakage scenarios

The initial fire profile of each scenario was presented in Fig. 5(b), and the detailed temperature contour near the orifice were plotted. In Scenario 1, leakage hole is located at Point A in the Electrolytic bath with the leakage direction of vertically upward. After leaking, hydrogen mixes with air and burns quickly, releasing a fire plume along the positive z axis as shown in Fig. 5(b). When the leaked gas reaches a height of 4 m, it begins to spread around with the highest temperature near the deck reaching 2259 K.

In Scenario 2, leakage hole is located at Point B at the Seawater desalination system. The leakage direction is horizontal along the positive x axis which is the downwind direction. It could be found that when the hydrogen fire is formed in a horizontal direction without fire extinguishing devices, the resulting high temperature is 1821 K which is lower than that of a vertical fire as shown in Fig. 5(b).

In Scenario 3, leakage hole is located at Point C at the Hydrogen storage tank I. The leakage direction is horizontal along the negative y axis which is perpendicular to the wind. In this scenario, the high-temperature gas quickly expands to the outside of the platform since the leakage hole is located close to the edge of the deck as shown in Fig. 5(b).

Affected by the wind, the flow direction of hydrogen will change after leakage occurs, from along the Y axis to along the X axis.

In Scenario 4, leakage hole is located at Point D at the Hydrogen storage tank II. The leakage direction is horizontal along the positive y axis. In this scenario, the leakage hole is located near the center of the platform, thus, there is almost no hydrogen flow out of the platform. Due to the obstruction congestion around the leakage point D, the flow of hydrogen is less affected by the wind direction compared to that of Scenario 3 as shown in Fig. 5(b).

#### Fire development of different leakage scenarios

Here, we presented the fire development during the non-premixed combustion of hydrogen fire in 100s. The combustion evolution behavior under each scenario in 3D space was shown in Fig. 6. Obviously, no matter where the leakage occurs, the high-temperature gas will extend to the upper deck around 10s. This is determined by the characteristic of low density of hydrogen, which leads to a rapid diffusion after leakage. Then, the high-temperature gas flow will spread around the upper deck, however, barely no elevated gas around the bottom deck. At the time of around 50s, the elevated hydrogen in each scenario begins to flow out of the platform, and after that, hydrogen continues to rise up and spread around. The highest combustion temperature is about 2400 K, and most of the high temperature areas are located about 3 m above the leakage hole.

**Table 1 – Hydrogen leakage scenarios setting.**

Leakage location	Leakage direction	Release velocity (m/s)	Flow rate (kg/s)
Point A	Positive along the z axis	30	0.491
Point B	Positive along the x axis	30	0.491
Point C	Negative along the y axis	30	0.491
Point D	Positive along the y axis	10, 30, 50	0.164, 0.491, 0.819

Analyzing the different fire in different scenario, it can be seen that the ambient wind may be an important factor influencing the flame's shape and the spreading direction of the fire. Moreover, the layout of the facility also plays an important role in the fire development. In Scenario 3, as the leakage hole is located near the edge of the platform, it can be seen that a large amount of hydrogen flows out of the platform, resulting in smaller coverage area of hydrogen thus causing less damage to the platform. However, in Scenario 4, as the leakage hole is located near the center of the platform, it has the biggest coverage area of high temperature.

#### Temperature evolution of key points during fire

In the simulation process, seven monitoring points were selected to observe the combustion evolution. The monitoring points are located as close as possible to the equipment nearby, so as to give a deduction of the danger caused by the high temperature to the equipment. The temperature curves of monitoring points during fire evolution are shown in Fig. 7.

It could be seen that, in Scenario 1 and Scenario 2, the temperatures of most monitoring points are below 600 K. Only the temperature of one monitoring point can reach 2000 K, i.e. monitoring point V (near the Hydrogen storage tank) in Scenario 1 and monitoring point II (near the Rectifier) in Scenario 2, respectively. In Scenario 3, the temperatures of most monitoring points are lower than 500 K, even the maximum temperature is only 1570 K, which demonstrates that this scenario is less dangerous than other scenarios. Moreover, the highest temperature of monitoring points appears in Scenario 4. Over half of the monitoring points can reach the temperature of 600 K, and the highest temperature even reaches 2340 K.

#### Combustion consequence

##### Simulation results of gas diffusion in fire

Considering the amount of generated water vapor can reflect the combustion level of hydrogen, the coverage of water vapor can also reflect the extent of diffusion of hydrogen. Thus, we presented the mole fraction contour of H<sub>2</sub> (0.1% mole fraction) and H<sub>2</sub>O (10% mole fraction) for different scenarios in Fig. 8. It could be seen hot water vapor i.e. 10% mole fraction of H<sub>2</sub>O accounts for a large proportion of the air composition in each combustion scenario. The sum of the two coverage areas is the real range of hydrogen transmission in the whole combustion process.

According to the mole fraction distribution in Fig. 8, it can be seen that the coverage area of hydrogen is mainly concentrated near the leakage hole, while that of water vapor is much larger. In this study, without considering the influence of intermediate products, it can be regarded as that the actual high-temperature area consists of two parts namely hydrogen covered area and hot water vapor covered area. Moreover, it can be seen from Fig. 8 that the distribution of mole fraction is almost consistent with that of high temperature (as shown in Fig. 9). However, a little difference appears in some regions, due to the incomplete combustion of hydrogen. To sum up, the development of high temperature area depends not only on the flow of hydrogen, but also on the diffusion of water vapor generated during combustion. Besides the region with high mole fraction of hydrogen, the temperature of the area with the mole fraction of water vapor higher than 10% will be higher than that of other areas with low mole fraction, which could be considered as an area with serious fire.

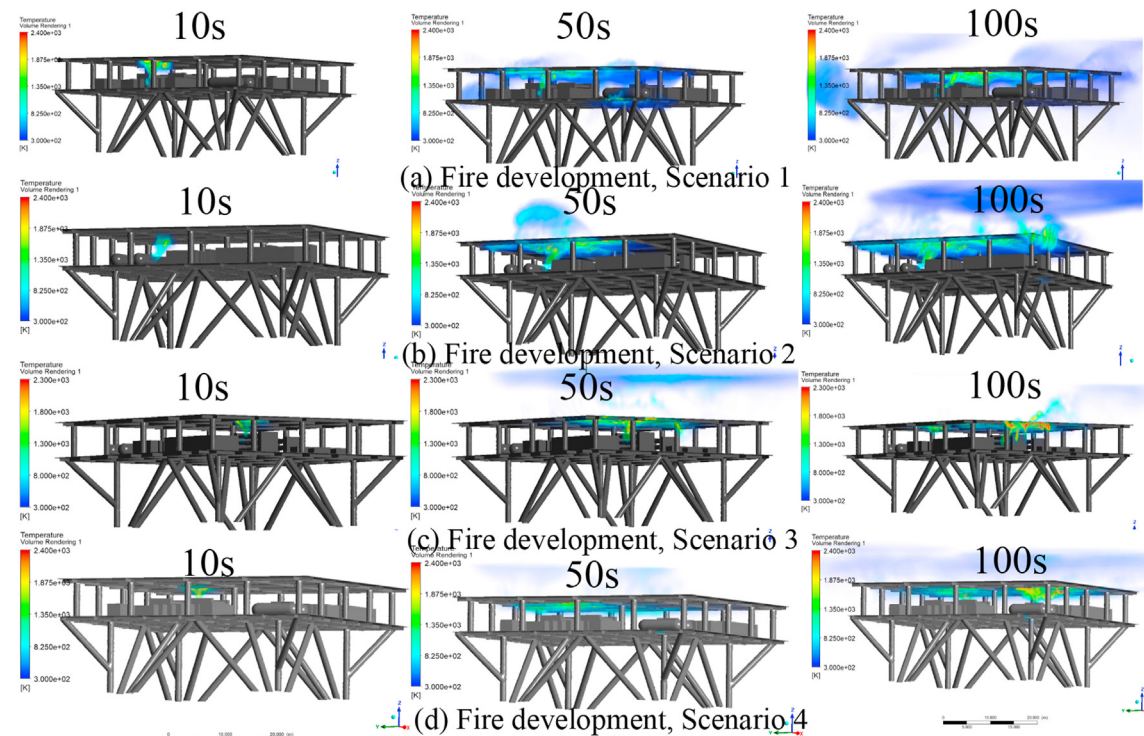
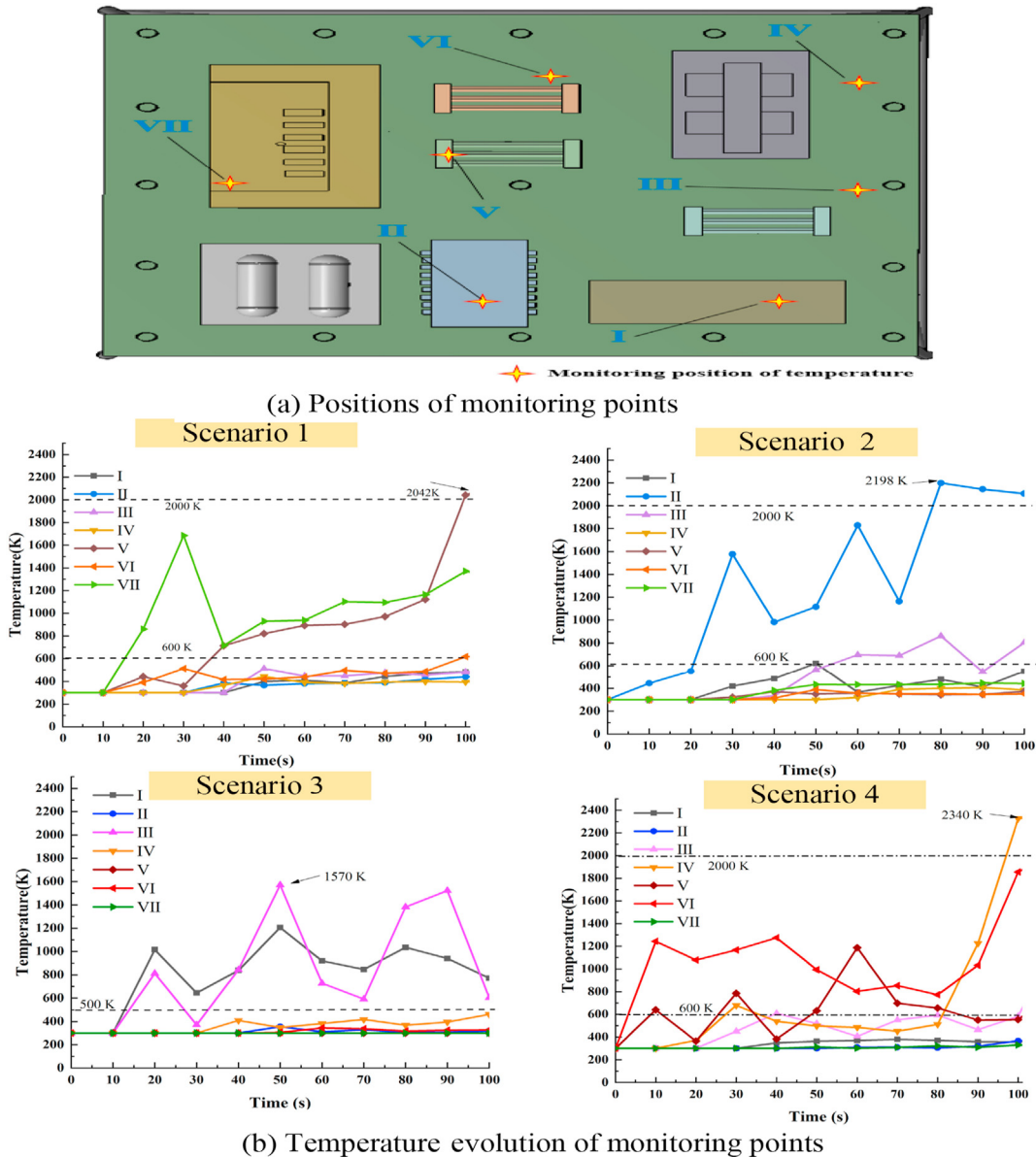


Fig. 6 – Combustion evolution of different fire scenarios.



**Fig. 7 – (a) Positions of monitoring points; (b) Temperature evolution of different monitoring points.**

The hazardous area of high temperature of different scenarios We draw the velocity streamline of the leaked gas in Fig. 9(a) to present the evolution of diffusion trajectory and velocity of hydrogen, when combustion behavior keeps stable at the end of the combustion of 100s. And also, we present the temperature contour of the slice crossing the ignition point to give a clear reflection of the distribution of temperature field on the platform as shown in Fig. 9(b). Through comparison, the flow trajectory of the leaked hydrogen gas is almost consistent with the high temperature area in the temperature contour.

In order to better reflect the diffusion of leaked hydrogen on the deck, the temperature profiles from the top view were presented in Fig. 9(c) for each scenario. It could be seen the most severe fire results appears in Scenario 4, which has the largest coverage area of high-temperature and the maximum peak temperature. This is due to the enough air which ensures

the sufficient combustion for the hydrogen. Moreover, a large amount of water vapor of high-temperature is produced, which leads to a large area covered by high-temperature gas.

It is well-known that ultra-high flame temperature produced in hydrogen fire could do great harms to human and surrounding facilities. Researches show that high-temperature resulting from combustible gas cloud will cause serious damage to human body [35]. According to the tolerance of people to the high temperature, dangerous areas can be divided into four levels from 333 K to 443 K [35], as shown in Table 2. As to steel structures, once the temperature exceeds 673 K, steel loses its strength significantly, which will cause serious damage to the platform structure [31]. However, considering that it takes a certain time for the structure to be heated up, thus, we take 443 K as the critical temperature to determine the hazardous area of hydrogen fire.

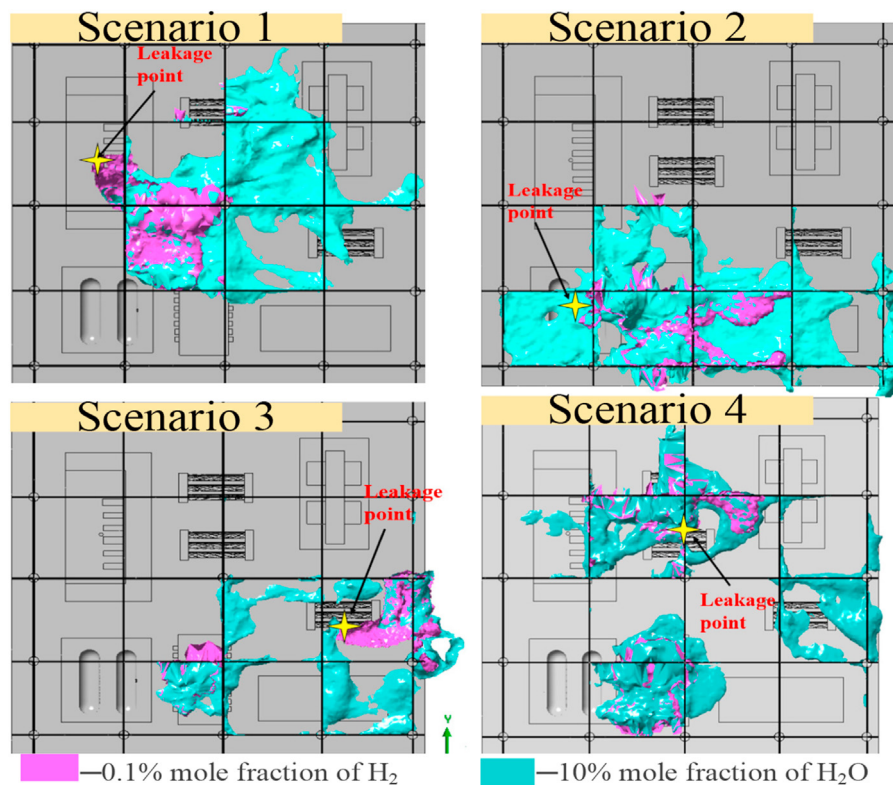
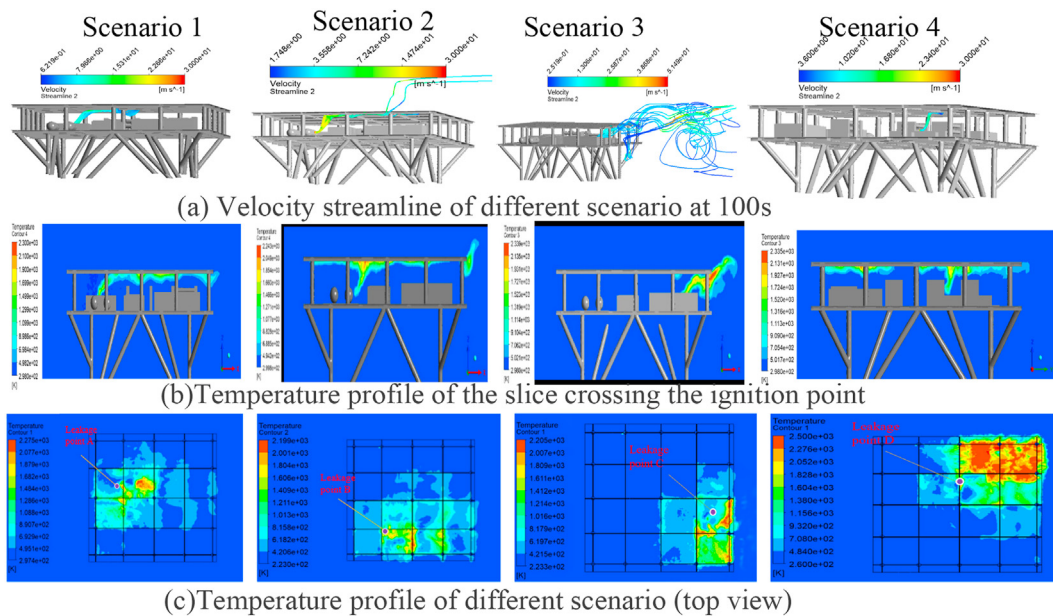
Fig. 8 – Distribution of mole fraction of H<sub>2</sub> and H<sub>2</sub>O.

Fig. 9 – Velocity streamlines and temperature fields of the slice crossing the ignition position at 100s.

According to the temperature results presented above, we get the size of the hazardous area of each scenario as shown in Table 3. It can be seen that Scenario 4 has the most serious results in combustion. Different leakage position will lead to a great change of the size of the hazardous area.

As it should be, when the equipment is exposed to fire for a long time, it will be heated to higher temperature due to

Table 2 – Classification for hazardous area.

Temperature range	>443 K	393 K–443 K	333 K–393 K	<333 K
-------------------	--------	-------------	-------------	--------

Danger level	High-risk	Medium-risk	Low-risk	Safe
--------------	-----------	-------------	----------	------

**Table 3 – Dimensions of hazardous areas over critical temperature of 443 K.**

Scenario	Length ( $X_{\max}$ )	Width ( $Y_{\max}$ )	Area
1	35 m	44 m	1190m <sup>2</sup>
2	43 m	32 m	1080m <sup>2</sup>
3	32 m	30 m	726m <sup>2</sup>
4	44 m	42 m	1328m <sup>2</sup>

thermal convection and thermal radiation. Thus, we take 673 K as the critical temperature to determine the Dangerous State of the equipment, which means that when the temperature is over 673 K it is regarded as Dangerous State and marked as D, while the Safety State is marked as S. From the result listed in Table 4, it could be found that the layout of facilities on the deck of platform has an impact on the damage caused by combustion, thus it could be concluded that by reasonably arranging the facilities, the loss can be reduced as much as possible in the case of a hydrogen fire.

#### Influence of leakage velocity on scenario 4

In this section we analyzed the influence of leakage velocity on combustion results. Since Scenario 4 has the most serious results in combustion, thus, we carried out the combustion simulations of this scenario under different leakage velocity including 10 m/s, 30 m/s and 50 m/s, respectively, while other conditions remain unchanged.

We presented the fire profiles at top view in Fig. 10(a). It could be seen that when the leakage velocity reduced to 10 m/s, the diffusion of hydrogen is obviously constrained in the space between two decks, resulting in the hazardous high-temperature range (over 443 K) reduced to 1/3 of that when leakage velocity of 30 m/s. When the velocity increases to 50 m/s, the covering area of the high temperature above 2000 K decreases, while the area covering from 443 K to 1600 K remains unchanged. This is because in the case of high leakage velocity, a large amount of unburned hydrogen concentrated inside the two decks of the platform due to incomplete combustion caused by insufficient oxygen. Although the increase of leakage velocity will lead to the increase of mole fraction of hydrogen, however combustion efficiency is almost the same as 30 m/s. The heat generated by combustion in some places with poor air circulation will even be reduced.

The dimensions of the areas at high temperature over 443 K for different leakage rate are listed in Table 5. It can be

seen that when the leakage velocity increased from 10 m/s to 30 m/s, the area of the high temperature over 443 K enlarged to 2.6 times. Moreover, when increased from 30 m/s to 50 m/s, the hazardous area almost unchanged.

Fig. 10(b) shows the temperature cures of key monitoring points with obvious fluctuation in Scenario 4. When the hydrogen leakage is at a lower velocity of 10 m/s, the temperature fluctuation of each monitoring point is less obvious and maintained stable at about 500 K during the 100s combustion process. When the leakage is at a higher velocity of 50 m/s, the temperature significantly increased and maintained stable at 600 K–1400 K during the late process of the combustion after 70s. In contrast to the results of leakage velocity of 30 m/s, the temperature of the monitoring point of 50 m/s starts to rise at 80s and reaches a new peak value at 100s.

To sum up, the leakage velocity has great influence on the final combustion results. Considering hydrogen is a combustible gas with explosive properties, when the leakage rate reaches 50 m/s, the incomplete combustion of hydrogen will have obvious effect on the temperature field results. The poorly ventilated space will easily lead to the accumulation of hydrogen and increase the risk of explosion. Moreover, it will also increase the affected area of hazardous temperature over 673 K, resulting in more facility damage.

#### Effects of firewall on hydrogen fire

The installation of firewall on offshore platform is an useful measure to protect key facilities from high temperature. The aim of this section is to examine the effectiveness of firewall on preventing the radiation of flames and transmission of high temperature gas during hydrogen combustion.

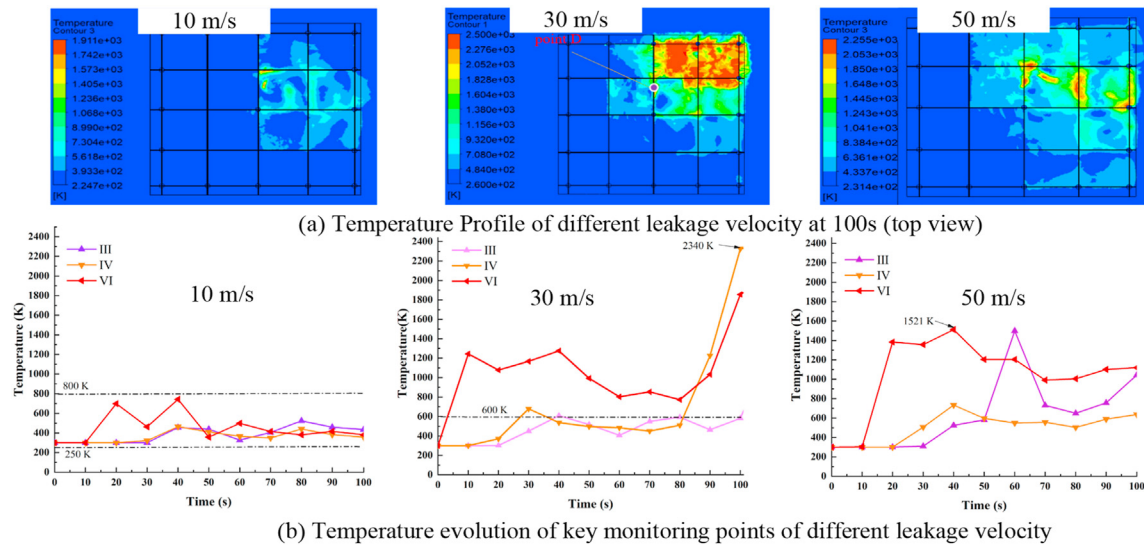
The combustion condition in scenario 4 is still selected for the analysis in this section. The firewall is constructed between the Compressor and Hydrogen storage tank with the size of  $L \times W = 15 \text{ m} \times 0.4 \text{ m}$ , as shown in Fig. 11(a). Considering the height of the firewall will play a key role on the protection effect, three different height is selected including 3 m, 4 m and 5 m, respectively.

Fig. 11 shows the geometric model of the firewall, the velocity streamline of hydrogen and the final temperature profile from top view according to different firewall conditions. From Fig. 11(b) it can be seen that obvious difference appears in the velocity streamline of the leaked gas after the firewall is installed. In this scenario, the firewall could prevent amount of hydrogen from flowing to the Compressor. Moreover, it can

**Table 4 – States of facilities in different fire scenarios.**

	Scenario 1	Scenario 2	Scenario 3	Scenario 4
Hydrogen storage tank I	S	S	D	S
Hydrogen storage tank II	D	S	S	D
Compressor	S	S	S	D
High voltage transformer	S	D	D	S
Rectifier	S	D	S	S
Seawater desalination system	D	D	S	S
Electrolytic bath	D	S	S	S

S-safe, D-dangerous



**Fig. 10 – Temperature evolution of key monitoring points of different leakage velocity.**

**Table 5 – Dimensions of hazardous areas over critical temperature of 443 K.**

Leakage velocity	Length ( $X_{\max}$ )	Width ( $Y_{\max}$ )	Area
10 m/s	22 m	30 m	506m <sup>2</sup>
30 m/s	44 m	42 m	1328m <sup>2</sup>
50 m/s	35 m	47 m	1321m <sup>2</sup>

be seen from the temperature field of the top view (Fig. 11(c)) that with the increase of the height of the firewall the area of high-temperature over 1500 K decreases significantly, thus it

can effectively protect the key facility from damage caused by high temperature.

Fig. 12 presents the temperature curves of key monitoring point III, IV, and VI. The results show that the maximum temperature of the three monitoring points has decreased from 2400 K to 2000 K after the firewall was constructed. The temperature in the first 30s is almost unchanged with the firewall installation. Compared with the case without firewall, the temperature around the Compressor has been obviously decreased. When the height of firewall is 5 m, it has the best protection effect, which can significantly reduce the ambient temperature to 1700 K around the Compressor.

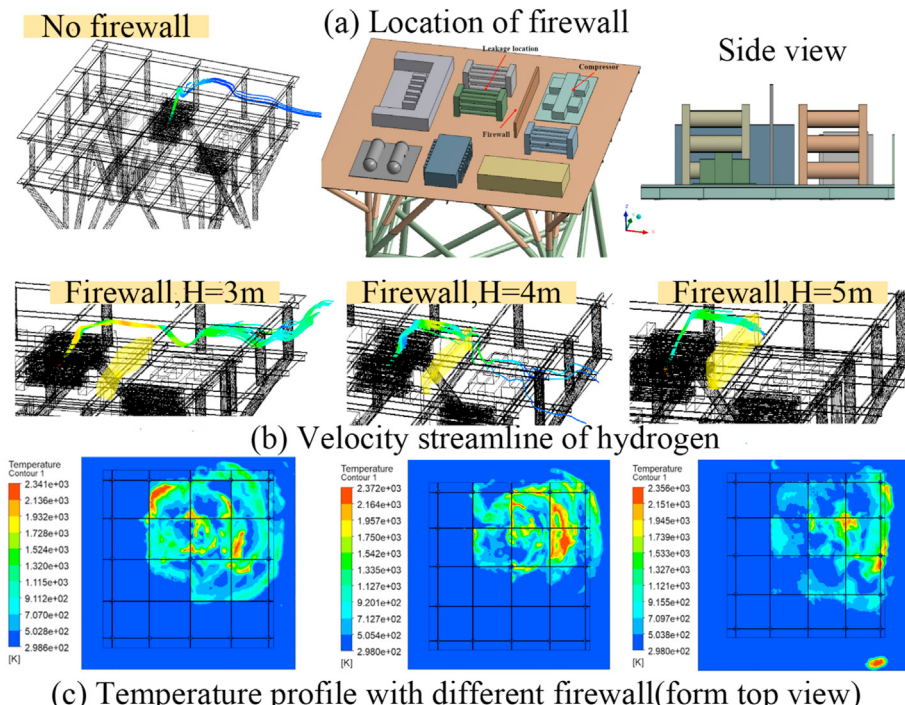


**Fig. 11 – (a)Location of firewall, (b) velocity streamline of hydrogen; and (c) temperature profile with different firewall.**

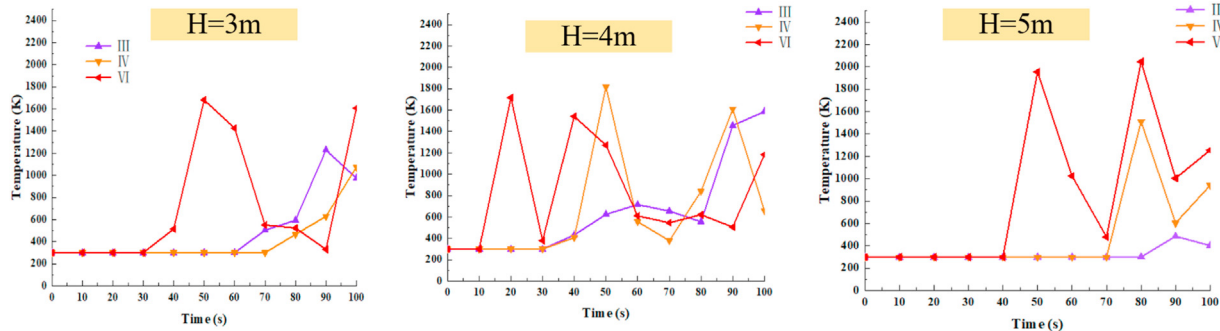


**Fig. 12 – Temperature evolution of monitoring points for different firewall.**

## Conclusion

This paper used the numerical method to investigate the hydrogen leakage and combustion behaviors in different fire scenarios on an offshore hydrogen production platform, based on CFD software ANSYS Fluent. Accidental fire scenarios are adopted and the fire evolution process is simulated and analyzed, and the impact of facilities layout, leakage position, leakage rate on the consequence of fire is assessed. Interesting results are derived from the simulations including the spatial distribution of high-temperature area on offshore platform, temperature variation characteristics of key positions and the state of each facility on the deck of platform. Meanwhile, the protection effect of firewall on facility is analyzed.

Due to the low density of hydrogen, after the leakage, hydrogen will concentrate near the deck and spread rapidly, reaching the edge of the platform in about 100s. The maximum combustion temperature can reach 2400 K. The layout of facilities on the platform has great influence on the diffusion of hydrogen. Poor ventilation condition appears when the leakage location is surrounded by more facilities, which may lead to potential explosion risk due to insufficient combustion of hydrogen. The difference of leakage velocity will affect the extent of hydrogen combustion. When the velocity is too high, the gas spreads faster, but the area covered by high temperature will decrease. Moreover, by constructing a firewall, it can block fire sources and thus protect facilities from high temperature. When the firewall is 5 m, the ambient temperature around the facility can be reduced to below 1700 K.

Hydrogen fire caused by leakage is an accident disaster that must be considered in advance of the hydrogen production on the offshore platforms. The findings reported in this study can be viewed as an useful method to predict the consequences of hydrogen combustion in case of accidental leakage. The results can provide some guidance for the facilities layout and will contribute to the safety design of offshore hydrogen production offshore platforms, and thus to promote the functional transformation of abandoned offshore platforms.

## Funding

This work was supported by the National Natural Science Foundation of China, China [grant numbers 51879272,

52111530036]; and the Fundamental Research Funds for the Central Universities, China [grant number 22CX03022A].

## Declaration of competing interest

The authors declare that they have no known competing financial interests or personal relationships that could have appeared to influence the work reported in this paper.

## R E F E R E N C E S

- [1] Moriarty P, Honnery D. Hydrogen's role in an uncertain energy future. *Int J Hydrogen Energy* 2009;34(1):31–9. <https://doi.org/10.1016/j.ijhydene.2008.10.060>.
- [2] Dunn S. Hydrogen futures: toward a sustainable energy system. *Int J Hydrogen Energy* 2002;27(3):235–64. [https://doi.org/10.1016/S0360-3199\(01\)00131-8](https://doi.org/10.1016/S0360-3199(01)00131-8).
- [3] Serna A, Tadeo F. Offshore hydrogen production from wave energy. *Int J Hydrogen Energy* 2014;39(3):1549–57. <https://doi.org/10.1016/j.ijhydene.2013.04.113>.
- [4] Ibrahim OS, Singlitico A, Proskovics R, McDonagh S, Desmond C, Murphy JD. Dedicated large-scale floating offshore wind to hydrogen: assessing design variables in proposed typologies. *Renew Sustain Energy Rev* 2022;160:112310. <https://doi.org/10.1016/j.rser.2022.112310>.
- [5] [https://www.toutiao.com/article/6974728317379428903/?tt\\_from=mobile\\_qq&utm\\_campaign=client\\_share&timestamp=164252275&app=news\\_article&utm\\_source=mobile\\_qq&utm\\_medium=toutiao\\_android&use\\_new\\_style=1&req\\_id=20220119001115010133166194143272E1&share\\_token=f058343d-0f04-4331-ae0d-99d38305b6f3&group\\_id=6974728317379428903&upstream\\_biz=toutiao\\_pc&source=m\\_redirect&wid=1657956656511](https://www.toutiao.com/article/6974728317379428903/?tt_from=mobile_qq&utm_campaign=client_share&timestamp=164252275&app=news_article&utm_source=mobile_qq&utm_medium=toutiao_android&use_new_style=1&req_id=20220119001115010133166194143272E1&share_token=f058343d-0f04-4331-ae0d-99d38305b6f3&group_id=6974728317379428903&upstream_biz=toutiao_pc&source=m_redirect&wid=1657956656511).
- [6] Aryai A, Abbassi R, Abdussamie N, et al. Reliability of multi-purpose offshore-facilities: present status and future direction in Australia. *Process Saf Environ Prot* 2021;148:437–61. <https://doi.org/10.1016/j.psep.2020.10.016>.
- [7] <https://news.bjx.com.cn/html/20200713/1088575.shtml>.
- [8] Froeling HAJ, Droge MT, Nane GF, et al. Quantitative risk analysis of a hazardous jet fire event for hydrogen transport in natural gas transmission pipelines. *Int J Hydrogen Energy* 2021;46(17):10411–22. <https://doi.org/10.1016/j.ijhydene.2020.11.248>.
- [9] Machniewski P, Molga E. CFD analysis of large-scale hydrogen detonation and blast wave overpressure in partially confined spaces. *Process Saf Environ Prot* 2022;158:537–46. <https://doi.org/10.1016/J.PSEP.2021.12.032>.

- [10] Mogi T, Kim D, Shiina H, Horiguchi S. Self-ignition and explosion during discharge of high-pressure hydrogen. *J Loss Prev Process Ind* 2007;21(2):199–204. <https://doi.org/10.1016/j.jlp.2007.06.008>.
- [11] Seo JK, Lee SE, Park JS. A method for determining fire accidental loads and its application to thermal response analysis for optimal design of offshore thin-walled structures. *Fire Saf J* 2017;92:107–21. <https://doi.org/10.1016/j.firesaf.2017.05.022>.
- [12] Li X, Chen G, Huang K, Zeng T, Zhang X, Yang P, et al. Consequence modeling and domino effects analysis of synergistic effect for pool fires based on computational fluid dynamic. *Process Saf Environ Prot* 2021;156:340–60. <https://doi.org/10.1016/j.psep.2021.10.021>.
- [13] Lin H, Luan H, Yang L, Han C, Karampour H, Chen G. A safety assessment methodology for thermo-mechanical response of offshore jacket platform under fire. *Process Saf Environ Prot* 2022;160:184–98. <https://doi.org/10.1016/j.psep.2022.02.007>.
- [14] Molkov V, Cirrone DMC, Shentsov V, et al. Dynamics of blast wave and fireball after hydrogen tank rupture in a fire in the open atmosphere. *Int J Hydron Energy* 2021;46(5):4644–65. <https://doi.org/10.1016/j.ijhydene.2020.10.211>.
- [15] Schefer RW, Houf WG, Bourne B, Colton J. Spatial and radiative properties of an open-flame hydrogen plume. *Int J Hydron Energy* 2006;31(10):1332–40. <https://doi.org/10.1016/j.ijhydene.2005.11.020>.
- [16] Swain MR, Filoso P, Grilliot ES, et al. Hydrogen leakage into simple geometric enclosures. *Int J Hydron Energy* 2003;28(2):229–48. [https://doi.org/10.1016/S0360-3199\(02\)00048-4](https://doi.org/10.1016/S0360-3199(02)00048-4).
- [17] Xiao J, Kuznetsov M, Travis JR. Experimental and numerical investigations of hydrogen jet fire in a vented compartment. *Int J Hydron Energy* 2018;43(21):10167–84. <https://doi.org/10.1016/j.ijhydene.2018.03.178>.
- [18] Schefer RW, Merilo EG, Groethe MA, Houf WG. Experimental investigation of hydrogen jet fire mitigation by barrier walls. *Int J Hydron Energy* 2011;36(3):2530–7. <https://doi.org/10.1016/j.ijhydene.2010.04.008>.
- [19] Giannissi SG, Hoyes JR, Chernyavskiy B, et al. CFD benchmark on hydrogen release and dispersion in a ventilated enclosure: passive ventilation and the role of an external wind. *Int J Hydron Energy* 2015;40(19):6465–77. <https://doi.org/10.1016/j.ijhydene.2015.03.072>.
- [20] Molkov V, Shentsov V, Brennan S, Makarov D. Hydrogen non-premixed combustion in enclosure with one vent and sustained release: numerical experiments. *Int J Hydron Energy* 2014;39(20):10788–801. <https://doi.org/10.1016/j.ijhydene.2014.05.007>.
- [21] Molkov V, Bragin M. Hydrogen-air deflagrations: vent sizing correlation for low-strength equipment and buildings. *Int J Hydron Energy* 2015;40(2):1256–66. <https://doi.org/10.1016/j.ijhydene.2014.11.067>.
- [22] Gu X, Zhang J, Pan Y, Ni Y, Ma C, Zhou W, et al. Hazard analysis on tunnel hydrogen jet fire based on CFD simulation of temperature field and concentration field. *Saf Sci* 2020;122:104532. <https://doi.org/10.1016/j.ssci.2019.104532>.
- [23] Takeno K, Okabayashi K, Kouchi A, et al. Dispersion and explosion field tests for 40MPa pressurized hydrogen. *Int J Hydron Energy* 2007;32(13):2144–53. <https://doi.org/10.1016/j.ijhydene.2007.04.018>.
- [24] Yuan Y, Wu S, Shen B. A numerical simulation of the suppression of hydrogen jet fires on hydrogen fuel cell ships using a fine water mist. *Int J Hydron Energy* 2021;46(24):13353–64. <https://doi.org/10.1016/j.ijhydene.2021.01.130>.
- [25] Kim E, Park J, Cho JH, Moon Il. Simulation of hydrogen leak and explosion for the safety design of hydrogen fueling station in Korea. *Int J Hydron Energy* 2013;38(3):1737–43. <https://doi.org/10.1016/j.ijhydene.2012.08.079>.
- [26] Schmidt D, Krause U, Schmidtchen U. Numerical simulation of hydrogen gas releases between buildings. *Int J Hydron Energy* 1999;24(5):479–88. [https://doi.org/10.1016/S0360-3199\(98\)00082-2](https://doi.org/10.1016/S0360-3199(98)00082-2).
- [27] Bauwens CR, Dorofeev SB. CFD modeling and consequence analysis of an accidental hydrogen release in a large scale facility. *Int J Hydron Energy* 2014;39(35):20447–54. <https://doi.org/10.1016/j.ijhydene.2014.04.142>.
- [28] Ouyang Y, He Q, Wang C, Shen Z. Numerical study of hydrogen/methane buoyant fires using FireFoam. *Int J Hydron Energy* 2020;45(24):13551–8. <https://doi.org/10.1016/j.ijhydene.2020.03.056>.
- [29] Houf WG, Evans GH, Schefer RW. Analysis of jet flames and unignited jets from unintended releases of hydrogen. *Int J Hydron Energy* 2009;34(14):5961–9. <https://doi.org/10.1016/j.ijhydene.2009.01.054>.
- [30] Kuroki T, Sakoda N, Shinzato K, et al. Temperature rise of hydrogen storage cylinders by thermal radiation from fire at hydrogen-gasoline hybrid refueling stations. *Int J Hydron Energy* 2018;43(5):2531–9. <https://doi.org/10.1016/j.ijhydene.2017.12.072>.
- [31] Willoughby DB, Royle M. The interaction of hydrogen jet releases with walls and barriers. *Int J Hydron Energy* 2011;36(3):2455–61. <https://doi.org/10.1016/j.ijhydene.2010.05.077>.
- [32] Yakhot V, Orszag S. Renormalization-group analysis of turbulence. *Phys Rev Lett* 1986;57(14):1722–4. <https://doi.org/10.1103/PhysRevLett.57.1722>.
- [33] Orszag SA, Yakhot V, Flannery WS, Boysan F, Choudhury D, Maruzewski J, et al. Renormalization group modeling and turbulence simulations. In: International conference on near-wall turbulent flows; 1993, 103146.
- [34] ANSYS, Inc. Ansys fluent theory guide. Canonsburg, PA, USA: Fluent Inc; 2021.
- [35] Fan D, Niu G, Li Z, Jia Q. The influence of relative wind speed on the smoke flow and temperature distribution in high-speed railway carriage fire. *Fire Sci Technol* 2022;41(9):7 [In Chinese], <http://www.cnki.com.cn/Article/CJFDTotai-XFKJ202209004.htm>.